HYDRAULIC AND THERMAL STUDIES ON A CHEVRON TYPE PLATE HEAT EXCHANGER

[1]Bhupal KUMAR, [2]S.N. SINGH*

[1]Research Scholar, Department of ME, IIT (ISM), Dhanbad, Jharkhand 826004, India

[*2]Associate Professor, Department of ME, IIT(ISM), Dhanbad. Jharkhand 826004, India

[*] Corresponding author; E-mail: snsingh631@yahoo.com

The present work deals with the experimental study of a single pass U-type chevron plate heat exchanger using liquid-liquid combination in both the channels for the range of Reynolds numbers, 800-5900. The influence of Reynolds number, pumping power and number of plates on the hydraulic and thermal performance of PHE are presented. Results are predicted for a chevron angle of $\beta=60^o$ and fixed port size d_p =25.4 mm for a different set of plates, namely, 15, 21 and 27 under two different conditions viz. (i) isothermal and (ii) non-isothermal. The present results of non-dimensional channel velocity and Nusselt number are compared with the analytical results of Bossiouny and Martin [3] and Nusselt number correlation of Wang and Sunden [19] respectively. At a Reynolds numbers of 3900, enhancement in Nusselt number on increasing number of plates from 15 to 21 and 21 to 27, is found to be 56% and 19% respectively. Based on experimental data, correlations for Nusselt number and friction factor are also developed.

Keywords: *Plate heat exchanger, flow maldistribution, chevron, pressure drop, Nusselt number*

1. Introduction

Plate heat exchangers, which were initially used for hygienic application such as dairy, brewery, pharmaceuticals and food processing industries, have now found their applications in the modern industry also. PHEs have quick response to control operations and possess capability to recover heat from extremely small temperature differences, thus widening their applications. In plate heat exchangers, the two plates facing each other have their corrugation lines alignment opposite to one another, so as to separate and produce cross corrugated flow channels. Gasket is present on one of the two mating surfaces. The fluid flow in each successive channel is in a direction opposite to the previous one. The cross-corrugated channel generates a highly turbulent flow, thus increasing the heat transfer even at low Reynolds number. The pressure drop as well as thermal performance of a plate heat exchanger depends critically on the distribution of fluid flow and geometrical properties of the chevron plates namely corrugation angle, area enlargement factor and channel aspect ratio.

Mueller and Chiou [1] presented a review of the problem related to maldistribution. Mulley and Manglik [2] experimentally investigated the turbulent flow heat transfer and pressure drop in a plate heat

exchanger for different corrugation angles. Their analysis is based on the assumption that flow rates are equal in all the channels. Bassiouny and Martin [3] derived the axial velocity, total pressure drop, flow distribution in channels and pressure distributions in inlet and outlet conduits of plate heat exchangers. They also developed a general flow maldistribution characteristic parameter, m^2, for inlet and exit port flows. Giraud et al. [4] experimentally studied the water vaporization inside a channel of a smooth plate-type heat exchanger at sub-atmospheric pressure. Fang et al. [5] investigated the flow distribution in manifolds of the heat exchanger. To predict the pressure distribution in headers, they proposed a discrete mathematical model matching the real physical phenomena. Tereda et al. [6] investigated the port-to-channel flow maldistribution for a fixed number of plates, and corrugation angle, varying only the port diameter. Tsai et al. [7] studied the hydrodynamic characteristics and distribution of flow in two cross-corrugated channels of PHEs. They also developed a 3D model with real size geometry of two cross-corrugated channels for the analysis of flow distribution. Gulenoglu et al. [8] experimentally studied the thermal and hydraulic performance of chevron type gasketed plate heat exchanger for three different plate geometries and developed a correlation for Nusselt number and friction factor. Faizal and Ahmed [9] has studied the pressure drop and heat transfer in PHE with different spacing between the corrugated plates. Han et al. [10], numerically and experimentally, investigated the temperature, pressure, and velocity fields in chevron corrugated-plate heat exchanger. They observed that the highest temperature appears around the upper port whereas the lowest temperature appears in the cold fluid inflow around the lower port. Fluid pressure in pressure field gradually reduced along the flow direction. Focke et al. [11] experimentally investigated effect of the corrugation inclination angle on the thermohydraulic performance of plate heat exchanger. They considered equal flow rate in each channel, thus indicating an ideal case of no flow maldistribution. Martin [12] considered combined effects of the longest flow path, and the disparity between cross and longitudinal flow, to derive an equation for the friction factor as a function of chevron angle and Reynolds number. Khan et al. [13] experimentally investigated the heat transfer for single phase flow in Reynolds numbers range (500 – 2500) for different chevron angles and corrugation depths. Nilpueng and Wongwises [14] investigated the heat transfer coefficient and pressure drop of a corrugated PHE at different surface roughness. Rao et al. [15] experimentally investigated the port flow maldistribution in PHEs for small and large plate packages at law corrugation angles, and found that the flow maldistribution increases with overall pressure drop. Rao and Das [16] experimentally studied the flow maldistribution and pressure drop across a plate heat exchanger. Fernandes et al. [17] studied flow characteristic in a corrugated type PHE for different corrugation angles and aspect ratios at low Reynolds number. They found that the friction factor increases either with the increase in aspect ratio or with the decrease in chevron angle.

The above cited literatures confirm that most of the researchers have considered the fluid distribution to be uniform, thus ignoring the flow maldistribution parameter. Moreover, no one has studied the hydraulic and thermal performance of a plate heat exchanger with respect to the pressure variation along the port, taking into consideration corrugation depth and pitch of the plate. Thus, the main objectives of the present study are to investigate the pressure distribution along the port with respect to the mass flow rate and number of channels. Heat transfer studies in terms of Nusselt number, overall heat transfer coefficient and effectiveness have also been carried out. Further, based on the experimental data,

correlations for convective Nusselt numbers and friction factor in the channels have been developed for a wide range of Reynolds number and Prandtl number.

2. Experimental Setup and Procedure

The layout of the experimental set-up as shown in Fig.1 consists of temperature transmitters 1,3,5 and 8, pressure transmitters 2,4,6, and 8, digital flow meters 9 and 10, primary PHE 11, secondary PHE 12, hot water tank 13, cold water tank 14, boiler water tank 15, boiler 16, ground water tank 17, pumps 18, 19, and 20, water treatment plant 21 and 22, pressure gauge 23, condenser 24, valves 25,26 and 27, and programmable logic control unit (PLC). White arrows in the figure depict the direction of flow of hot fluid while the dark arrows depict the direction of flow of cold fluid. Fig. 2 presents the flow arrangement of a U-type PHE. PID (proportional integral derivative) temperature controller regulates the temperature in Secondary PHE (12) to obtain the desired hot water temperature. Secondary PHE (12) as shown in Fig. 1, consists of a maximum of 27 plates. Investigation of the flow distribution is carried out for 15 plates (14 channels), 21 plates (20 channels) and 27 plates (26 channels) from the first to last channel. Digital flow meters (9&10), with a maximum deviation of 2.0% from the standard flow meter, and four PT-100 thermometers (1,3,5 & 8), with a maximum deviation of 1% from the standard thermometer, are provided in hot and cold fluid streams.

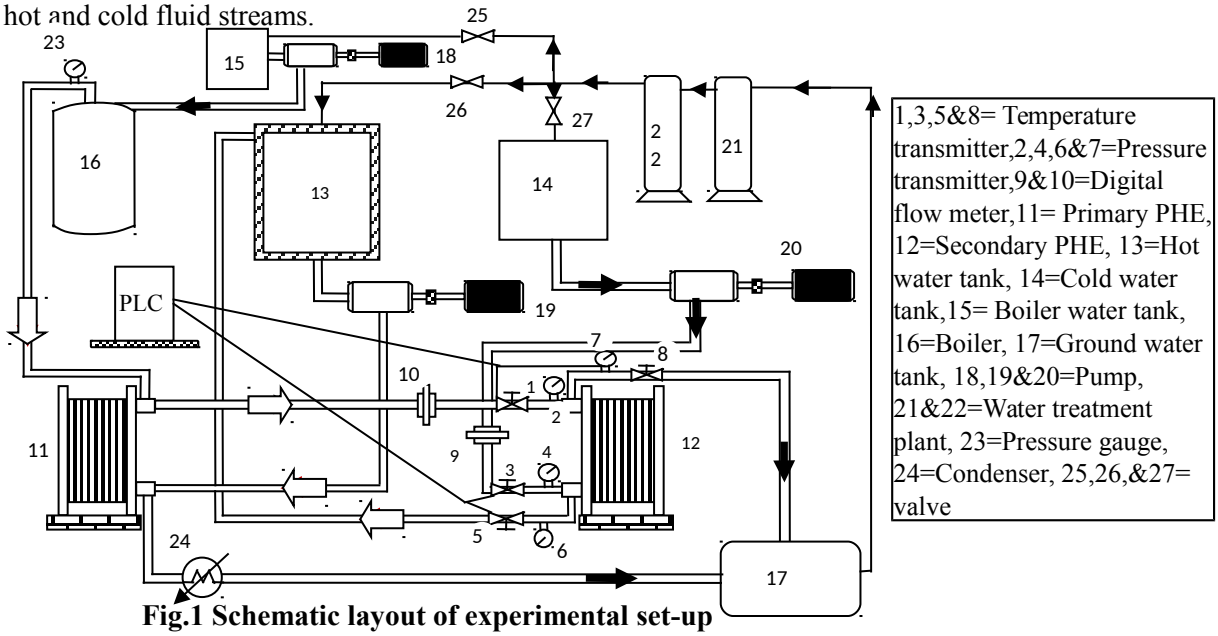

Fig.1 Schematic layout of experimental set-up

The maximum operating steam pressure and temperature of boiler are 7.5 bars and 160°C. Steam enters in primary PHE at 2 bars and 135°C, heating the water to desired temperature. This heated water is used in secondary PHE to heat the water coming from the cold-water tank. Steam after leaving the primary PHE condenses in the condenser. Thermometers are placed near to the ports of PHE in the stainless-steel pipe section at the inlet and outlet of fluid streams. Four pressure transmitters (2,4,6 & 7), calibrated with a standard pressure meter and with an uncertainty of ±0.25%, are provided near the inlet and outlet port of cold and hot fluid streams. Flow rates of the working fluid (demineralized water) being pumped by pumps (19 & 20), is controlled by speed of the pump. Digital flow meters (turbine type flow meter), pressure transmitters and thermometers are connected to a Programming Logic Controller (PLC), which is further

connected to a Human Interface unit (HMI). PLC measures and controls the temperatures, pressure and flow rates of hot and cold fluid streams.

In addition to this, pressure transmitters (range: 0 -500 kPa) having a copper tube are used to measure the pressure drop along the channels. The typical connection of this tube acting as a pressure tap with the experimental chevron plate is shown in Fig. 3.

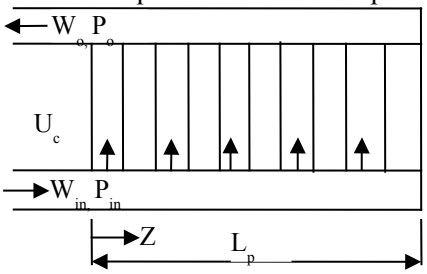

Fig. 2 Flow arrangement for U type PHE

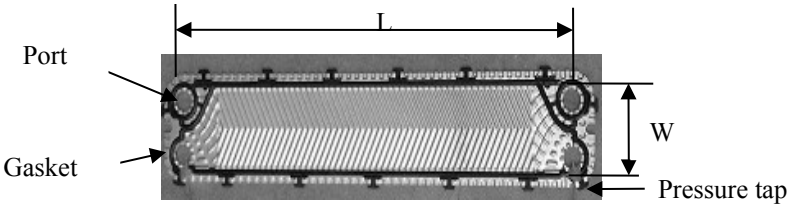

Fig. 3 Pressure tap fixed at top and bottom port of the tasted plate of PHE

3. Data reduction

3.1. Hydraulic analysis

Enlargement factor is calculated using the following equation developed by Mehrabian and Poulter [20]

$$\phi = \frac{1}{p_c}\int_0^{p_c}\sqrt{1+(\frac{\pi p}{p_c})^2\cos^2(\frac{2\pi x}{p_c})}dx \tag{1}$$

Pressure drop due to friction in the corrugated passage is calculated using the following empirical formula:

$$\Delta p_{ch} = f_{ch}\frac{L_{ch}}{d_h}\rho\frac{v^2_{chm}}{2} \tag{2}$$

Maldistribution parameter, m^2, is calculated using Bossiouny and Martin's [3] equation for identical inlet and exit port dimension

$$m^2 = (\frac{nA_c}{A_p})^2\frac{1}{\zeta_c} \tag{3}$$

Non-dimensional channel velocity is obtained by using the expression developed by Rao et al. [15]

$$u_c = (\frac{\Delta p_{ch}}{\Delta p_{mch}})^{\frac{1}{2-a}} \tag{4}$$

Results obtained from equation 4 are compared with the analytical results of Bossiouny and Martin [3] for U-type flow arrangement, stated as:

$$u_c = (\frac{A_p}{nA_c})m\frac{\cosh m(1-z)}{\sinh m} \tag{5}$$

3.2. Thermal analysis

For adiabatic heat exchanger;

$$Q = h_h A \Delta T_h = h_c A \Delta T_c \quad (6)$$

Overall heat transfer coefficient is obtained from:

$$Q = UA \Delta T_m \quad (7)$$

Experimental results of Nusselt number are compared with the correlational values of Nusselt number developed by Wang and Sunden [19] for gasketed chevron type plate heat exchanger, stated as:

$$Nu = 0.205 \mathrm{Pr}^{1/3} (\frac{\mu}{\mu_w})^{1/6} \{f \mathrm{Re}^2 \sin(180 - 2\beta)\}^{0.374} \quad (8)$$

Pump power is calculated by,

$$P_p = \dot{m} \Delta p_t / \rho \quad (9)$$

3. The uncertainty in measurements

Uncertainties in measurement of the flow rate, pressure drop, friction factor and Reynolds number, are calculated from Moffat [18] procedure. Uncertainties in flow rate, pressure, and temperature measurement are found to be ±2%, ±0.25% and ±0.25% respectively. Maximum uncertainties in the Reynolds number, friction factor, and Nusselt number are obtained as ±3.9%, ±4.7%, and ±9.5% respectively.

5. Results and Discussion

5.1 Validation

5.1.1 *Comparison of experimental non-dimensional channel velocity with Bossiouncy and Martin [3] analytical model of three different sets of PHE*

Comparison between experimental non-dimensional channel velocity with the analytical model of Bossinouny and Martin [3], for three different sets of PHE, is shown in Fig.4. It shows that experimental results are in good agreement with the theoretical model. The presence of small deviations is due to the sudden change in cross-sectional area of the inlet and outlet ports. Channel pressure drop in successive channels keep on decreasing. Hence, non-dimensional channel velocity also decreases. For higher number of plates, deviation of channel pressure drop from the mean value is higher. Thus, maximum non-uniformity is obtained for 27 set of plates.

5.1.2 *Comparison of experimental Nusselt number with previous published correlations of Nusselt number*

Fig. 5 illustrates a comparative study between the experimental Nusselt number and Wang and Sunden's correlation of Nusselt number [19] for gasketed chevron type plate heat exchanger. The experimental results are found to be in good agreement with published results. Slight variation in results are attributed to the surface behavior and laboratory atmospheric conditions. Higher flow rates promote turbulent flow in the channel which enhances the thermal characteristics. Hence, Nusselt number is found to be greater at higher Reynolds number.

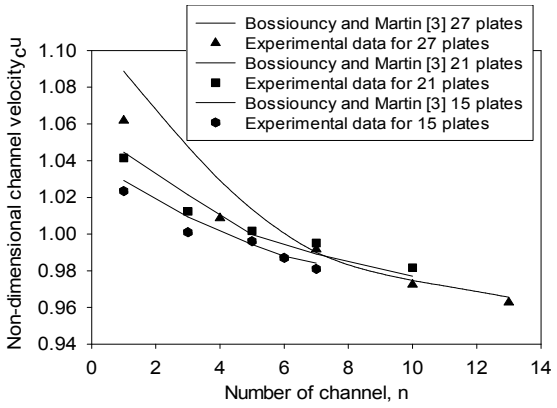

Fig. 4 Comparison of experimental non-dimensional channel velocity with Bossiouncy and Martin [3] analytical model of three different sets of PHE

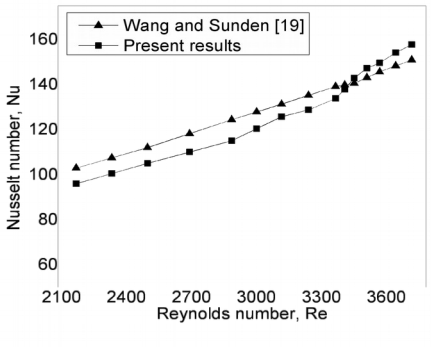

Fig. 5 Comparison of present correlated Nusselt number with Wang and Sunden [19] correlation

5.2. Typical experimental results

5.2.1 *Variation of static pressure along the inlet and outlet ports*

Fig. 6 shows the variation of static pressure along the ports in 15 plates set PHE for different mass flow rates. It is observed that the static pressure increases along both the ports. The total pressure (sum of dynamic and static pressures) at inlet, for a particular flow rate, remains constant. The fluid dynamic pressure along the inlet port decreases due to flow channeling effect as a result of which static pressure tends to increase. On the contrary, the fluid flow rate increases along the outlet port due to increase in flow rate between channels, resulting in increase of dynamic, and thus decrease in static pressure along the port. This leads to a strong pressure drop in the channel. Static pressure at inlet as well as outlet increases with the increase in mass flow rate due to channeling effect.

Fig.7 shows the variation of static pressure along the ports in 27 set of plates for different mass flow rates. Inlet and outlet pressure profiles follow the same trend along the port as in the earlier case. Increase in the number of plates lead to the formation of more channels, which eventually results in higher flow branching. Higher flow branching causes larger momentum changes. For the larger number of plates, momentum gain due to the decrease in mass flow rate is higher than the friction and turn around losses, leading to increase in inlet pressure along the port. On the other hand, pressure in the outlet port gradually decreases due to higher momentum and friction losses for large number of plates. Thus, channel pressure drop and pressure difference at inlet and outlet port is higher for the larger number of plates.

Fig. 8 shows variation of static pressure along the inlet port for different number of plates at the same mass flow rate. Static pressure along the inlet port increase due to increase in the friction losses. Static pressure for 27 plates set is much lower in comparison to 15 and 21 plates set. This is because of the fact that the higher number of channels are formed for larger plates set which results in higher flow branching**,** thus causing smaller momentum changes.

Variation of static pressure along the outlet port for different number of plates at the same mass flow rate is shown in Fig. 9. For smaller number of plates, the pressure variation is found to be higher than that for larger number of plate set. This is due to the higher flow branching in larger plates set. Increase in

number of plates is also accompanied by higher frictional losses. Thus, flow maldistribution reduces with decrease in number of plates.

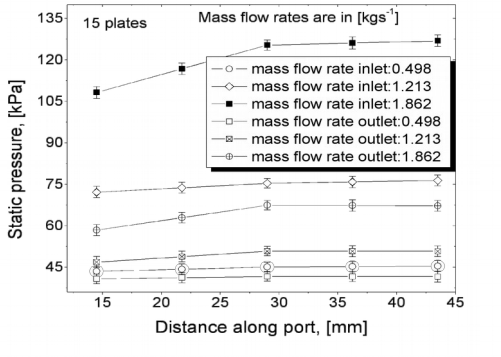

Fig. 6 Variation of static pressure along the port for 15 plates at different mass flow rate

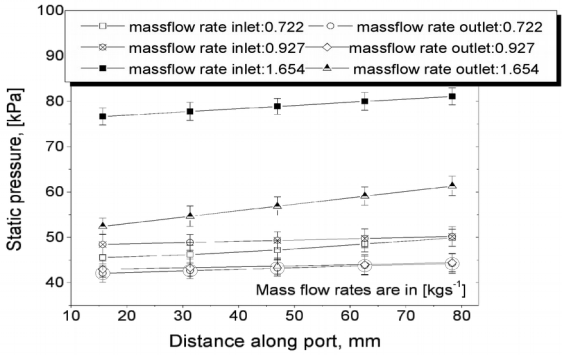

Fig. 7 Variation of static pressure along the port for 27 plates at different mass flow rate

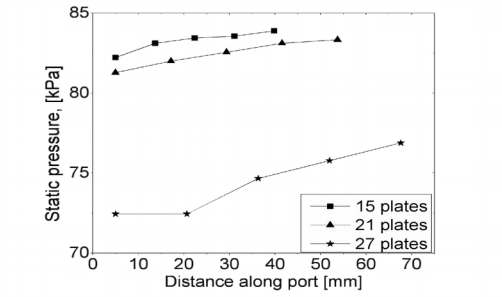

Fig. 8 Variation of static pressure of inlet port at constant mass flow rate (1.57 kg/s)

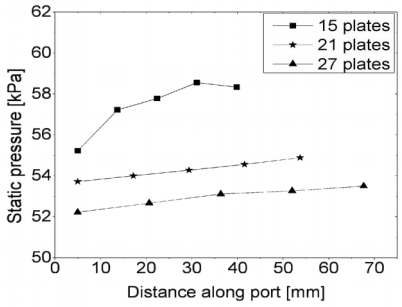

Fig. 9 Variation of static pressure of outlet port at constant mass flow rate (1.57 kg/s)

5.2.2 *Variation of static pressure along the port for isothermal and non-isothermal condition*

Variation of static pressure drop along the inlet port for isothermal and non-isothermal conditions for different sets of plates is shown in Fig. 10. The static pressure profile for both conditions shows a similar trend. It can be observed that due to the rise in temperature of the working fluid, static pressure for non-isothermal condition is higher. Thermal content of water decreases due to the heat lost to the surface of plate. This results in depletion of the fluid enthalpy, further causing a gradual drop of pressure in comparison to the isothermal test. Fluid between the plates of heat exchanger expands with increase in temperature of plates. The inner surface of the plates restricts the expansion of fluid as a result of which, pressure between the plates increases enormously even for a slight increase in temperature. Thus, for the same flow rate, higher pressure drop is observed for the hot fluid stream as compared to cold fluid stream.

Fig.11 shows the pressure profile along the outlet port for different set of plates at both, isothermal and non-isothermal conditions. It is observed that due to the increase in outlet port velocity, static pressure increases along the port for all the conditions. For the same mass flow rate, static pressure for smaller set is higher as compared to the larger set of plates. This is due to the port velocity which decreases with

increase in number of plates. Under non-isothermal condition, as the temperature increases, density of fluid decreases, velocity increases, and hence static pressure increases.

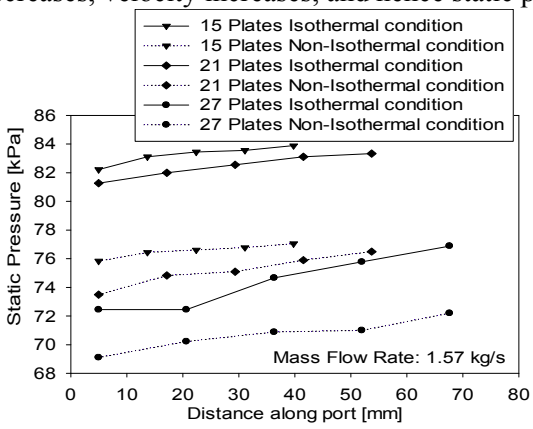

Fig. 10 Variation of static pressure along the inlet port at isothermal and non-isothermal condition

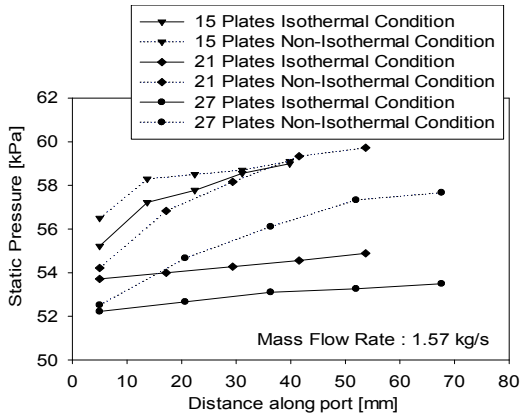

Fig. 11Variation of static pressure along the outlet port at isothermal and non-isothermal condition

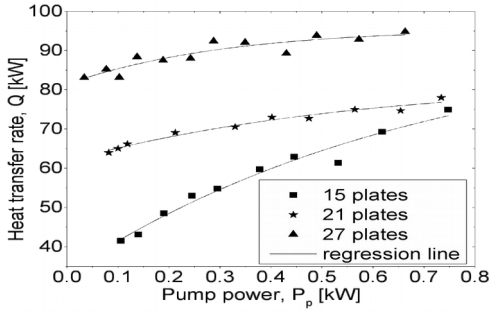

Fig. 12 Variation of heat transfer rate with pump power

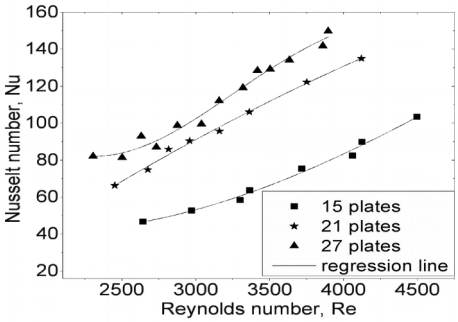

Fig. 13 variations of Nusselt number with Reynolds number

5.2.3 *Variation of heat transfer rate with pump power for different sets of plate*

Variation of heat transfer rate with pump power for different sets of plate is shown in Fig. 12. Heat transfer through the plates increases with increase in pumping power. High pumping power increases the flow rate of fluid resulting in high turbulent motion of the fluid molecules. This directly increases convective heat transfer through the fluid in channels of PHE. Therefore, heat transfer increases as the pumping power is increased. In larger sets of plates, availability of larger surface area for heat transfer leads to higher heat exchange at same pumping power. Higher surface area increases the probability of interaction of the fluid molecule with plate surface, thus leading to the higher heat losses.

5.2.4 *Variation of Nusselt number with Reynolds number for different sets of plates*

Fig.13 presents the variation of Nusselt number with Reynolds number for different sets of plate. It shows that the Nusselt number increases with increase in Reynolds number. Higher flow rates give rise to random molecular motion, resulting in higher convective heat transfer. Therefore, Nusselt number increases with increase in mass flow rate. Due to flow channeling effect, mass flow rate in a particular

channel decreases with increase in number of plates, resulting in lower heat transfer through the channel. However, for the larger set of plates, there is an increase in the overall heat transfer surface area which results in the increase of Nusselt number.

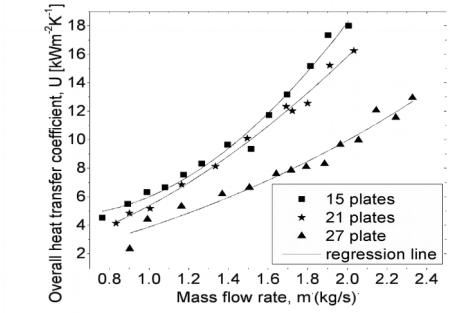

Fig.14 variation of overall heat transfer coefficient with mass flow rate

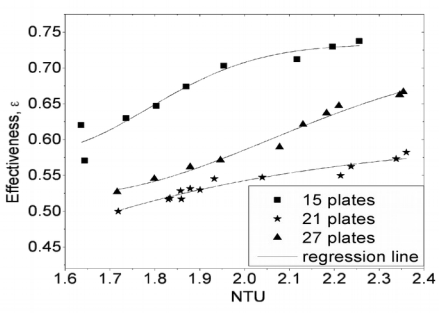

Fig. 15 Variations of effectiveness with NTU

5.2.5 *Variation of overall heat transfer coefficient with mass flow rate in PHE for different sets of plates*

Variation of overall heat transfer coefficient with mass flow rate for different sets of plates is presented in Fig. 14. Overall heat transfer coefficient increases with increase in mass flow rate. This is due to the increase in the difference of hot fluid temperatures, and decrease in LMTD. At higher flow rates, convective heat transfer is also higher. As flow rate increases, motion of fluid becomes highly irregular with the fluid particles moving to and fro in all the directions. Higher fluid mixing enhances the heat transfer, thus increasing the overall heat transfer coefficient. At the same mass flow rate, due to increase in the channel flow velocity, overall heat transfer coefficient for 15 set of plates is higher than that of 27 set of plates.

5.2.6 *Variation of effectiveness with NTU in PHE for different sets of plates*

Variation of effectiveness with number of transfer units in PHE for different sets of plates are shown in Fig. 15. It shows that the effectiveness increases with increase in the number of transfer units. This is due to the fact that the higher mass flow rate increases the overall heat transfer coefficient. Thus, 15 plates set gives satisfactory results as compared to the other higher number of plates set. At a given NTU, effectiveness increases with decrease in the number of plates due to low value of m^2. On the other hand, an increase in the number of plates increases m^2, thus deteriorating performance of the PHE.

5.2.7 *Variation of flow maldistribution parameter with mass flow rate of different sets of plates*

Variation of flow maldistribution parameter with mass flow rate is shown in Fig 16. It is observed that the flow maldistribution parameter increases with increase in mass flow rate for the fixed port size. This is attributed to the fact that the overall friction resistance decreases at higher mass flow rates. It is also seen that the flow maldistribution parameter (m^2), is higher for larger number of plates. More channels are formed for a larger number of plates which result in higher flow branching. This further leads to larger momentum changes. Momentum gain due to decrease in flow rate is higher for a large number of

plates, which ultimately leads to higher inlet pressure along the port. On the other hand, pressure in the outlet decreases gradually due to higher momentum and friction losses for a large number of plates. As a result, flow maldistribution parameter is higher for a large number of plates.

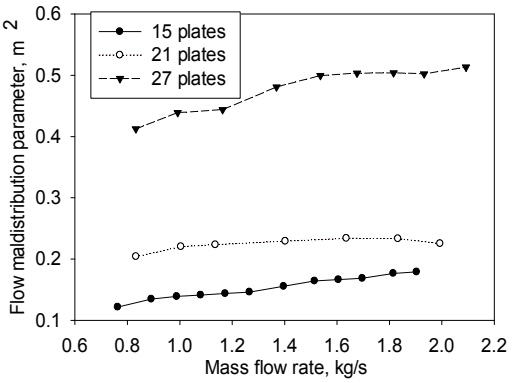

Fig. 16 Variation of flow maldistribution parameter with mass flow rate

6. Correlations

Based on the experimental data, correlations for the channel friction factor and Nusselt number are developed as follows.

$$f_{ch} = 2.573\,\mathrm{Re}^{-0.1513} \qquad 800 \le \mathrm{Re} \le 4300 \tag{10}$$

$$Nu = 0.097\,\mathrm{Re}^{0.453}\,\mathrm{Pr}^{2.139} \qquad 2100 \le \mathrm{Re} \le 4500 \tag{11}$$

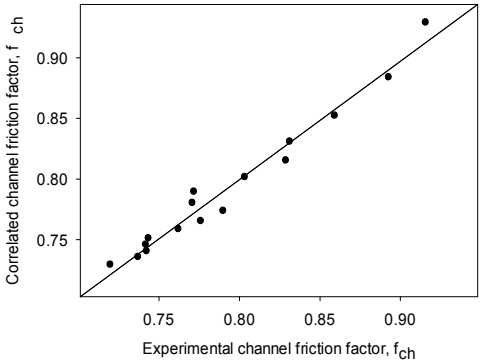

Fig. 17 Parity plot of channel friction factor

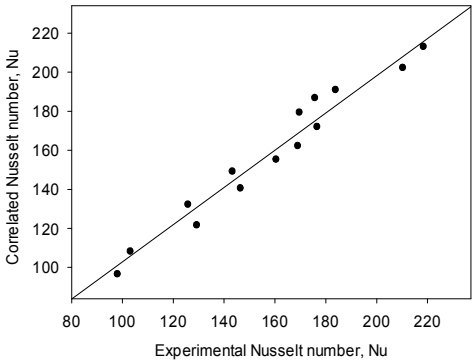

Fig. 18 Parity plot of Nusselt number

Comparing equation 10 with generalized formula for friction factor, $f = CRe^{-a}$, *we* get C=2.73 and a= -0.1513.

The above correlation of channel friction factor shows that channel friction factor decreases with the increase in Reynolds number. Convective Nusselt number, which is a strong function of Re and Pr, increases with an increase in the Reynolds and Prandtl numbers. Correlation coefficient for the above correlation is 0.98 which signifies an excellent agreement between the correlated and experimental data as shown in the parity plot (Figs.17 & 18).

7. Conclusions

Pressure drop and heat transfer from port to channel for three different sets of plates in a PHE are experimentally investigated under isothermal and non-isothermal steady state conditions. Effects of Reynolds number and number of plates on pressure drop and flow maldistribution have been studied. For the same mass flow rate, static pressure increases along the inlet and outlet ports but channel pressure drop decreases. The pressure drop in the channel decreases with increase in number of plates in PHE. Higher flow maldistribution is observed for non-isothermal working condition. Nusselt number is found to be increasing with Reynolds number and number of plates. Overall heat transfer coefficient increases with Reynolds number, but decreases with an increase in number of plates. It is observed that the heat transfer increases with pumping power. Thus, the conventional practice of designing PHE considering flow distribution to be uniform for a large number of plates is not desirable.

Nomenclature

A	heat transfer area [m^2]	A_p	cross- sectional area of the port [mm^2]
A_c	cross- sectional area of the channel [mm^2]	a	exponent of the Reynolds number ($f = CRe^{-a}$)
b	plate spacing [mm], $p+t$,	c_p	fluid specific heat at constant pressure [$Jkg^{-1}\,^oC^{-1}$]
D_h	hydraulic dia of corrugated channel, $2b/\varphi$	d	diameter of port, 25.4 mm
f_{ch}	channel friction factor	h	convective heat transfer coefficient [$Wm^{-2}\,^oC^{-1}$]
k	fluid thermal conductivity [$Wm^{-1}\,^oC^{-1}$]	L	vertical distance between the two ports, 650 mm
L_p	port length [mm]	L_{ch}	length of channel [mm]
m^2	flow maldistribution parameter	Nu	Nusselt number, hD_h / k,
n	number of channels per fluid	Pr	Prandtl number, $\mu\, c_p / k$
p	pitch of the plate [mm]		
p_c	wavelength	P_p	Pump power [W]
p_{in}	inlet port pressure [Pa]	p_o	outlet port pressure [Pa]
p_t	total pressure drop in PHE [Pa]	Δp_{ch}	channel pressure drop
Δp_{mch}	mean channel pressure drop	Re	number, $\rho u_c D_h / \mu$
Q	rate of heat transfer between fluids, [W]	Q_{max}	rate of heat transfer [W]
T	Temperature, [^oC]	$T_{m,c}$	cold bulk mean temperature [^oC]
$T_{m,h}$	hot bulk mean temperature [^oC]	ΔT_m	logarithmic mean temperature difference [^oC]
T_m	bulk mean temperature [^oC]	t	thickness of plate, 0.5 mm
U	overall heat transfer coefficient [$Wm^{-2}\,^oC^{-1}$]	u_c	dimensionless channel velocity
V_{chm}	mean channel velocity [ms^{-1}]	W	width of the plate, 108 mm
W_{in}	inlet port velocity [ms^{-1}]	W_o	outlet port velocity [ms^{-1}]
Z	axial co-ordinate along the port [mm]	z	dimensionless co-ordinate along the port, Z/L_p
PHE	plate heat exchanger		

Greek letters

β	corrugation angle of the plate (60^o)	φ	area enlargement factor
ρ	density of the fluid [kgm^{-3}]	μ	dynamic viscosity of fluid [Pa s]
ζ_c	overall friction coefficient (fL/d_h +other miner losses, including turning losses)		

ε effectiveness

References

[1] Mueller, A.C., Chiou, J.P., Review of Various Types of Flow Maldistribution in Heat Exchangers, *Heat Transfer Engineering*, 9 (1988), 2, pp. 36-50

[2] Muley, A., Manglik, R.M., Experimental Study of Turbulent Flow Heat Transfer and Pressure Drop in Plate Heat Exchanger with Chevron Plates, *ASME Journal of Heat Transfer*, 121 (1999), 1, pp. 110–117

[3] Bassiouny, M.K., Martin, H., Flow distribution and pressure drop in plate heat exchangers-I, *Chem. Eng. Sci*., 39 (1984), pp. 693-700

[4] Giraud, F., Toublanc, C., Rullière, R., Bonjour, J., Clausse, M., Experimental study of water vaporization occurring inside a channel of a smooth plate-type heat exchanger at subatmospheric pressure, *Applied Thermal Engineering* 106 (2016), pp. 180–191–

[5] Lu F., Luo Y.H., Yang S.M., Analytical and Experimental Investigation of Flow Distribution in Manifolds for Heat Exchangers, *Journal of Hydrodynamics*, 20 (2008), 2, pp.179-185

[6] Tereda, F.A., Srihari, N., Sunden, B., Das, S.K., Experimental Investigation on Port-to-Channel Flow Maldistribution in Plate Heat Exchangers, *ASME Journal of Heat Transfer Engineering*, 28 (2005), 5, pp. 435-443

[7] Tsai, Y.C., Liu, F.B., Shen, P.T., Investigation of pressure drop and flow distribution in a chevron-type plate heat exchanger, *International Communications in Heat and Mass transfer*, 36, (2009), pp. 574-578

[8] Gulenoglu, C., Akturk, F., Aradag, S., Uzol, N.S., Kakac, S., Experimental Comparison of performance of three different plates for gasketed plate heat exchangers, *International Journal of Thermal Science*, 75 (2014), pp. 249-256

[9] Faizal, M., Ahmed, M.R., Experimental Studies on a Corrugated Plate Heat Exchanger for Small Temperature Difference Applications, *Experimental Thermal and Fluid Science*, 36 (2012), pp. 242-248

[10] Han, X.H., Cui, L.Q., Chen, S.J., Chen, G.M., Wang, Q., A numerical and experimental study of chevron, corrugated-plate heat exchangers, *International Communications in Heat and Mass Transfer*, 37 (2010), pp. 1008-1014

[11] Focke, W.W., Zachariades, J., Olivier, I., The effect of the corrugation inclination angle on the thermohydraulic performance of plate heat exchangers, *International Journal of Heat and Mass Transfer*, 28 (1985), 8, pp. 1469-1479

[12] Martin, H., A theoretical approach to predict the performance of chevron-type plate heat exchangers, *Chemical Engineering and Processing,* 35 (1996), pp. 301-310

[13] Khan, T.S., Khan, M.S., Chyu, M.C., Ayub, Z.H., Experimental investigation of single phase convective heat transfer coefficient in a corrugated plate heat exchanger for multiple plate configurations, *Applied Thermal Engineering,* 30 (2010), pp. 1058–1065

[14] Nilpueng, K., Wongwises, S., Experimental study of single-phase heat transfer and pressure drop inside a plate heat exchanger with a rough surface, *Experimental Thermal and Fluid Science*, 68, (2015), pp. 268–275

[15] Bobbili, P.R., Sunden, B., Das, S.K., An experimental investigation of the port flow maldistribution in small and large plate package heat exchangers, *Applied Thermal Engineering*, 26 (2006), pp.1919-1926

[16] Bobbili. P.R., Das, S.K., An experimental study on the influence of flow maldistribution on the pressure drop across a plate heat exchanger, *ASME Journal of Fluid Engineering,* 126 (2006), pp. 680-691

[17] Fernandes, C.S., Dias, R.P., Nóbrega, J.M., Maia, J.M., Laminar flow in chevron-type plate heat exchangers: CFD analysis of tortuosity, shape factor and friction factor, *Chemical Engineering and Processing,* 46 (2007), pp. 825–833

[18] Moffat, R.J., Describing the uncertainties in experimental results, *Experimental Thermal and Fluid Science*, 3 (1988), pp. 3-11

[19] Wang, L., Sunden, B., Optimal design of plate heat exchangers with and without pressure drop specifications, *Applied Thermal Engineering*, 23 (2003), pp. 295–311

[20] Mehrabian, M.A., Poulter, R., Hydrodynamics and thermal characteristics of corrugated channels: computational approach, *Applied Mathematical Modelling*, 24 (2000), pp. 343-364